

Study of the Reaction $\pi^- p \rightarrow \rho^0 n$ at 15 GeV/c*

F. Bulos, R. K. Carnegie, G. E. Fischer, E. E. Kluge, D. W. G. S. Leith,
H. L. Lynch, B. Ratcliff, B. Richter, H. H. Williams, and S. H. Williams
Stanford Linear Accelerator Center, Stanford University, Stanford, California 94305

and

M. Beniston
IBM, Palo Alto, California 94304
(Received 5 March 1971)

We present the results of a wire spark-chamber experiment studying the reaction $\pi^- p \rightarrow \pi^+ \pi^- n$ at 15 GeV/c. The differential cross section, π - π mass distribution, and density-matrix elements have been determined from 10 000 $\pi\pi n$ events ($M_{\pi\pi} < 1.0$ GeV) produced with $-t < 0.30$ (GeV/c)². Both the density-matrix elements and the differential cross section exhibit structure in the forward direction ($-t < m_\pi^2$).

We report the results of a wire spark-chamber experiment performed at the Stanford Linear Accelerator Center to study the reaction $\pi^- p \rightarrow \pi^+ \pi^- n$ at an incident beam momentum of 15 GeV/c.¹ This reaction has been previously studied at lower energies,² but prior to this experiment no accurate determinations of the density-matrix elements or the differential cross section $d\sigma/dt$ have been available at high energies ($t \equiv$ momentum transfer squared to the nucleon). In addition, knowledge of these quantities for very small momentum transfers has been lacking at all energies. Absorption models³ and also the vector-dominance model (VDM)⁴ predict that the $\pi^- p \rightarrow \rho^0 n$ differential cross section for transversely polarized ρ mesons should have a sharp rise in the forward direction ($-t < m_\pi^2$) as does the reaction $\gamma N \rightarrow \pi^* N$. A detailed comparison of the data with VDM is given in the Letter immediately following this one.⁴

The experimental apparatus is described in detail elsewhere.⁵ The momentum of the incident π^- was determined to an accuracy of $\pm 0.3\%$ and the horizontal and vertical projected π^- angles at the target were determined to an accuracy of ± 0.5 mrad by counter hodoscopes placed in the beam line. The spectrometer, which measured the momenta and angles of the outgoing pions, consisted of seven two-gap spark chambers, an analyzing magnet ($100 \times 38 \times 120$ cm³ aperture), and trigger hodoscopes. Three chambers were placed upstream from the magnet and four downstream. The inside faces of the magnet gap were

lined with scintillation counters to veto events in which a particle intersected the pole faces. The trigger logic required an incident beam particle, two or more charged particles downstream of the magnet, and no signal from the magnet veto counters. In addition, scintillator-Pb sandwich counters surrounded the 1-m-long liquid H₂ target to detect particles which escaped the spectrometer. A gas Cherenkov counter placed downstream of the spectrometer distinguished π 's from heavier particles. The information from both the Cherenkov and the target counters was used only in the off-line analysis.

Because the main pion beam passed through the spectrometer system, and because of the high instantaneous fluxes ($8 \pi^-$ per 1.6- μ sec burst), a small region of the chambers was desensitized by the installation of a polyurethane plug. As a result, very asymmetric ρ decays could not be observed.^{6,7} This limitation of the plug was matched by the low-momentum cutoff of the magnet which also prohibited observation of very asymmetric decays. For $|\cos\theta| < 0.8$ (where θ is the polar angle of the π^- in the helicity frame⁷), the average acceptance was 25% and varied slowly as a function of $M_{\pi\pi}$ and t for ρ - n events. The π - π mass resolution was less than ± 10 MeV at the mass of the ρ ; the missing-mass resolution was ± 80 MeV, and the t resolution was calculated to be $\pm 0.016(-t)^{1/2}$ (GeV/c)².

The density-matrix elements of the di-pion system were determined as a function of t by fitting the observed decay angular distribution by the form $\omega(\theta, \varphi) = W(\theta, \varphi)E(\theta, \varphi)$, where

$$W(\theta, \varphi) = (1/4\pi) [1 + (\rho_{00} - \rho_{11})(3 \cos^2\theta - 1) + 2\sqrt{3} \operatorname{Re}(\rho_{0s}) \cos\theta - 3\sqrt{2} \operatorname{Re}(\rho_{10}) \sin 2\theta \cos\varphi - 2(6)^{1/2} \operatorname{Re}(\rho_{1s}) \sin\theta \cos\varphi - 3\rho_{1-1} \sin^2\theta \cos 2\varphi] \quad (1)$$

is the angular distribution for S and P waves, $E(\theta, \varphi)$ is the detection efficiency of the spectrometer, and θ and φ are the polar and azimuthal decay angles, respectively, of the π^- in the ρ rest frame. The normalization of the density-matrix elements was $\rho_{00} + 2\rho_{11} + \rho_{00}^S = 1$. The analysis was performed on the events in the mass interval $0.665 < M_{\pi\pi} < 0.865$ GeV. A Monte Carlo program was used to calculate $E(\theta, \varphi)$ to correct for geometrical losses. By refitting the data with more restrictive geometrical cutoffs than those imposed by the apparatus, it was ascertained that the ρ_{ij} obtained were not affected by the geometry of the apparatus. The density-matrix elements ρ_{ij}^H (helicity frame) and ρ_{ij}^J (Jackson frame) were obtained and their consistency checked by rotating from one frame to the other. By varying the missing-mass cutoff and using the information from the target counters, it was determined that $(12 \pm 2)\%$ of the event sample were N^* events and that this contribution did not affect the values of ρ_{ij} .

The density-matrix elements are shown in Figs. 1(a)-1(e). The error bars shown are statistical only; systematic errors, which could result if there were small unknown biases in the apparatus or event reconstruction, are estimated to be less than the statistical errors. The fact that $\text{Re}\rho_{0S}$ and $\text{Re}\rho_{1S}$ do not vanish is conclusive evidence that the di-pion system may not be described by a pure P wave. We conclude that partial waves with $l \geq 2$ are not required to describe the decay angular distribution since there are no systematic deviations of the fit from the data in any particular region of $\cos\theta, \cos\varphi$.⁸

Many of the density-matrix elements exhibit structure for momentum transfers less than m_π^2 ; in particular, there is a striking dip in $\rho_{00} - \rho_{11}$ for $-t < \frac{1}{2}m_\pi^2$, a region which has not been studied in previous experiments. A narrow dip in $\rho_{00} - \rho_{11}$ is predicted by one-pion-exchange absorption (OPEA) models.³

It is not possible to determine separately ρ_{11} or ρ_{00}^S from the angular distribution alone; however, the Schwartz inequalities⁹ on the helicity amplitudes and the requirement that the diagonal elements of the density matrix be positive definite enable one to establish limits on ρ_{00}^S and ρ_{11} . The limits on ρ_{11} calculated in this manner are shown in Fig. 1(f).

Independent information on ρ_{00}^S (and hence ρ_{11}) may be obtained from the existing $\pi^- p \rightarrow \pi^0 \pi^0 n$ data.¹⁰ The curve in Fig. 1(f) shows the values of ρ_{11} calculated assuming $d\sigma(S \text{ wave})/dt \propto |t|e^{7t}(t$

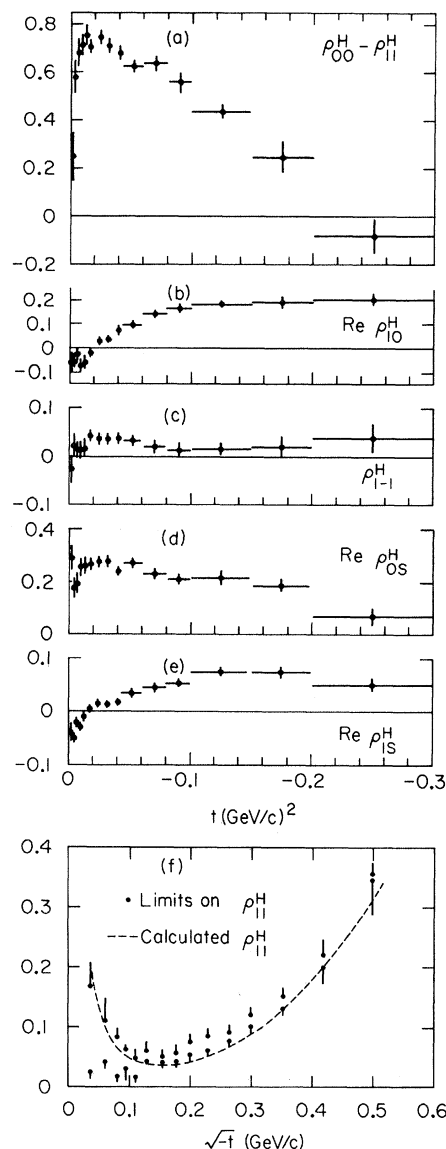


FIG. 1. (a)-(e) The density-matrix elements in the helicity frame for $0.665 < M_{\pi\pi} < 0.865$ GeV. The error bars indicate the statistical errors. (f) The upper and lower limits on ρ_{11} which are determined from the Schwarz inequalities on the helicity amplitudes and the requirement that the diagonal density-matrix elements be positive definite. The errors on the limits result from the propagation of the errors on the density-matrix elements. The curve is the calculated value of ρ_{11} obtained when the amount of S wave is estimated from the $\pi^- p \rightarrow \pi^0 \pi^0 n$ data.

$-m_\pi^2)^{-2}$, which is a good representation of the t dependence of the $\pi^0 \pi^0$ data for $-t \geq \frac{1}{4}m_\pi^2$. For smaller values of $-t$, the $\pi^0 \pi^0$ data are not sufficient to determine the shape of the differential cross section. However, the form $|t|e^{At}(t-m_\pi^2)^{-2}$ is the shape of the S -wave cross section which is

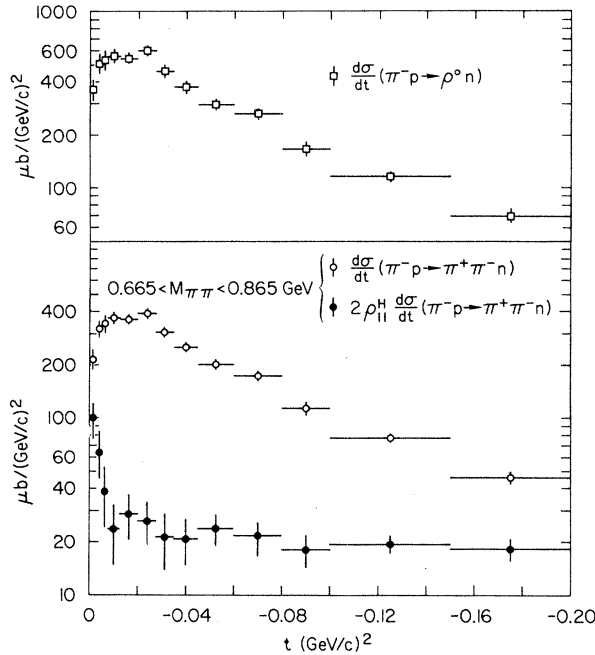


FIG. 2. The total and transverse differential cross sections as functions of momentum transfer for $\pi^- p \rightarrow \pi^+ \pi^- n$, $0.665 < M_{\pi\pi} < 0.865$ GeV, and the total differential cross section for $\pi^- p \rightarrow \rho^0 n$. The error bars indicate the statistical errors.

predicted by OPEA.³ The normalization was obtained by scaling the $\pi^0\pi^0$ cross section to 15 GeV.¹¹ The values of ρ_{11} obtained in this manner are consistent with the limits described above. We have also calculated ρ_{11} taking the amount of S wave from our fits to the $\pi-\pi$ mass spectrum (see discussion below) and assuming the same t dependence as above. The results obtained agree within errors.

A peak in the calculated value of ρ_{11} is observed in the forward direction [Fig 1(f)]. The structure does not strongly depend on the details of the S-wave t dependence; for example, if the S wave is assumed to decrease by only 25% from $t = -m_\pi^2$ to $t = t_{\min}$, rather than vanishing as predicted by OPEA, the peak in ρ_{11} is decreased by only 20%.

The total differential cross section $d\sigma(\pi^- p \rightarrow \pi^+ \pi^- n)/dt$ and the transversely polarized cross section $2\rho_{11}^H d\sigma(\pi^- p \rightarrow \pi^+ \pi^- n)/dt$ are shown in Fig. 2 for the mass interval $0.665 < M_{\pi\pi} < 0.865$ GeV. The error in the overall normalization is $\pm 5\%$ and results from uncertainties in the counter and spark-chamber efficiencies, thick-target corrections, and track reconstruction efficiency. Our measurements of $d\sigma(\pi^- p \rightarrow \pi^- p)/dt$ with the same apparatus agree with those of Foley *et al.*¹² to

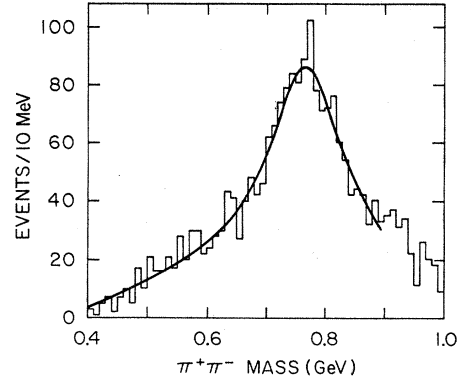


FIG. 3. The observed $\pi^+\pi^-$ mass spectrum for $|t| < 0.02$ (GeV/c)². The curve represents the fit described in the text, after it has been folded with the acceptance.

within 2%. The sharp rise in the transverse cross section and the dip in the total cross section are predicted by OPEA models and verify the fact that the reaction is dominated by pion exchange for small momentum transfers. The total ρ differential cross section, which is also shown in Fig. 2, has been obtained from the $\pi^+\pi^-$ cross section by subtracting the amount of S wave and correcting for the fraction of the ρ mass spectrum outside our mass interval. The normalization error is $\pm 25\%$, the dominant contribution coming from the uncertainty in the ρ line shape.

The $\pi-\pi$ mass distribution shown in Fig. 3 is described from 0.4 to 0.9 GeV using only a P-wave resonance and an S-wave background. The P wave is parametrized by a Breit-Wigner form which was used by Pišut and Roos¹³ to fit both ρ^- and ρ^0 mass distributions at lower energies:

$$\frac{d\sigma}{dm} \propto \frac{1}{q} \frac{m^2 m_0^2 \Gamma_l^2(m)}{(m_0^2 - m^2)^2 + m_0^2 \Gamma_l^2(m)} \int_{t_{\min}(m)}^T e^{At} dt,$$

where l is the angular momentum of the resonance and

$$\Gamma_l(m) = \Gamma_0 \left(\frac{q}{q_0}\right)^{2l+1} \frac{m_0}{m} \frac{1 + R^2 q_0^2}{1 + R^2 q^2},$$

$$q = (\frac{1}{4}m^2 - m_\pi^2)^{1/2}, \quad q_0 = (\frac{1}{4}m_0^2 - m_\pi^2)^{1/2}.$$

Here m_0 and Γ_0 are mass and width parameters, respectively, A is the slope of $d\sigma(\pi^- p \rightarrow \rho^0 n)/dt$, $t_{\min}(m)$ is the kinematical lower limit of t , T is the upper limit of $|t|$ for the event sample, and R is a parameter which corresponds to the range of the interaction. The S-wave contribution is also parametrized by the above form with an assumed mass and width of 0.7 GeV and 0.4 GeV,

respectively; this is consistent with the $\pi^0\pi^0$ mass distribution.¹⁰ The fit yields the ρ parameters $M_\rho = 0.771 \pm 0.004$ GeV and $\Gamma_\rho = 0.160 \pm 0.014$ GeV, and $R^2 = 4.8 \pm 3.2$ (GeV/c)⁻². The amount of S wave required is $(11 \pm 2)\%$ which agrees well with the 12% predicted by scaling the $\pi^0\pi^0n$ data.¹¹ Other acceptable fits to the mass spectrum may also be obtained by changing R or by choosing different Breit-Wigner functions, such as the standard P -wave form discussed by Jackson.¹⁴ Although these forms are indistinguishable within the interval 0.4-0.9 GeV, the high-mass behavior results in normalizations differing by $\pm 20\%$. Since this region is complicated by the presence of other resonances, it is difficult to distinguish between the forms by extending the fits to higher masses.

We summarize our results as follows: The dipion density-matrix elements have been determined as functions of t for $0.665 < M_{\pi\pi} < 0.865$ GeV and exhibit pronounced structure at small momentum transfers. We note that the angular distribution is well described by S and P waves alone. The differential cross sections for $\pi^-p \rightarrow \rho^0n$ and $\pi^-p \rightarrow \pi^+\pi^-n$ for the above mass interval have also been determined. The total and longitudinal cross sections show a dip at small t , whereas the transverse cross section has a strong forward peak.

*Work supported by the U. S. Atomic Energy Commission.

¹These results supersede the preliminary data presented by F. Bulos *et al.*, in Proceedings of the Fifteenth International Conference on High Energy Physics, Kiev, U. S. S. R., 1970 (Atomizdat., Moscow, to be published).

²J. A. Poirier *et al.*, Phys. Rev. **163**, 1462 (1967); B. D. Hyams *et al.*, Nucl. Phys. **B7**, 1 (1968); P. B. Johnson *et al.*, Phys. Rev. **176**, 1651 (1968); J. P. Baton and G. Laurens, Phys. Rev. **176**, 1574 (1968); W. Selove *et al.*, Phys. Rev. Lett. **21**, 952 (1968); J. H. Scharenguivel *et al.*, Phys. Rev. Lett. **24**, 332 (1970). Additional references may be found in these papers.

³K. Gottfried and J. D. Jackson, Nuovo Cimento **34**, 735 (1964); G. L. Kane and M. Ross, Phys. Rev. **177**, 2353 (1969); F. Henyey *et al.*, Phys. Rev. **182**, 1579 (1969); P. K. Williams, Phys. Rev. D **1**, 1312 (1970).

⁴See F. Bulos *et al.*, following Letter [Phys. Rev. Lett. **26**, 1457 (1971)], for a list of references on VDM.

⁵G. T. Armstrong *et al.*, SLAC Report No. SLAC-PUB-801, 1970 (unpublished).

⁶When viewed from the helicity frame those events with $|\cos\theta| > 0.85$ (where θ is the polar angle of the π^-) were not observed by the apparatus. In the Gottfried-Jackson frame, events with $|\cos\theta|$ as large as 0.95 were observed.

⁷The helicity frame is defined as the ρ rest frame in which $-\hat{z}$ is along the direction of the outgoing neutron and \hat{y} is normal to the production plane.

⁸A more detailed discussion of whether partial waves with $l \geq 2$ are present is given in F. Bulos *et al.*, SLAC Report No. SLAC-PUB-884, 1970 (unpublished), along with tables of the density-matrix elements.

⁹For example: $\text{Re}\rho_{05}^2 \leq \rho_{00}\rho_{00}^S$; $\text{Re}\rho_{10}^2 \leq \rho_{00}\rho_{11}$; $\text{Re}\rho_{15}^2 \leq \rho_{11}\rho_{00}^S$; $|\rho_{1-1}| \leq \rho_{11}$.

¹⁰P. Sonderegger and P. Bonamy, in Proceedings of the Fifth International Conference on Elementary Particles, Lund, Sweden, 25 June-1 July 1969 (unpublished); E. I. Shibata, D. H. Frisch, and M. A. Wahlig, Phys. Rev. Lett. **25**, 1227 (1970).

¹¹The $\pi^0\pi^0n$ data were scaled according to p^{-2} where p is the incident beam energy. Sonderegger and Bonamy (Ref. 10) have shown that this scaling works well over a range of 3 to 18 GeV/c. It has been assumed that the $\pi^0\pi^0$ cross section has $l=0$.

¹²K. J. Foley *et al.*, Phys. Rev. **181**, 1775 (1969).

¹³J. Pišut and M. Roos, Nucl. Phys. **B6**, 325 (1968).

¹⁴J. D. Jackson, Nuovo Cimento **34**, 1644 (1964).